The magnetic gradient tensor: Its properties and uses in source characterization

P.W. SCHMIDT and D.A. CLARK, CSIRO Industrial Physics, Lindfield NSW, Australia

Airborne magnetic surveys have improved dramatically over the past three decades with advances in both data acquisition and image processing techniques. Magnetic surveys form an integral part of exploration programs and are now routinely undertaken before geological mapping programs. These advances have been made despite treating the magnetic field as a scalar, wherein various processing procedures that assume a potential field are compromised. If the vector information could be retrieved, either by direct measurement or by mathematical manipulation, magnetic surveys could be improved even further. For instance, the total magnetic intensity (TMI) could be corrected so it represents a true potential field.

Vector surveys, where the direct measurement of vector components has been attempted, have met with mixed success. The accuracy of direct measurement of the field vector is largely governed by orientation errors, which for airborne platforms are so large that the theoretical derivation of the components from the TMI is actually preferable. For this reason, and others listed below, it is desirable to measure the field gradient(s) rather than the field vector.

We discussed the calculation of vector components and magnetic moments from the TMI in previous articles (Schmidt and Clark, 1997; Schmidt and Clark, 1998) which compare theoretical derivations with laboratory measurements and demonstrate the validity of the approach. Phillips (2005) has since taken these ideas further by using a moving window to generalize the technique to tackle larger areas, and also to search for sources with specified directions of magnetization. This article is largely drawn from, and updates, an earlier contribution of ours (Schmidt and Clark, 2000).

Gradient measurements are relatively insensitive to orientation. This is because gradients arise largely from anomalous sources, and the background gradient is low. This contrasts with the field vector, which is dominated by the background field, i.e., arising from the earth's core. Gradient measurements are therefore most appropriate for airborne applications. Another advantage is they obviate the need for base stations and corrections for diurnal variations. They also greatly reduce the need for regional corrections, which are required by TMI surveys because of deeper crustal fields that are normally not of exploration interest, or the normal (quasi-) latitudinal intensity variation of the global field.

Gradient measurements also provide valuable additional information, compared to conventional total field measurements, when the field is undersampled. Undersampling is common perpendicular to flight lines in airborne surveys, is usual in ground surveys, and always applies in downhole surveys. Conditions under which calculation is preferable to measurement of vectors and gradient tensors have yet to be characterized by modeling and case studies. Synergistic interpretation of calculated vectors and measured gradients may allow significantly more information to be extracted from airborne surveys.

Advantages of determining gradients in general. The advantages of magnetic gradient surveys include:

- Better resolution of shallow features and closely spaced sources
- Better definition of structural features
- Suppression of regional anomalies due to deep sources
- Mapping of subvertical contacts
- Tighter anomalies around compact sources
- Easier detection and delineation of pipe-like sources
- Constraining of local strike direction*
- Determination of which side of a line the source lies*
- Common mode rejection of geomagnetic variations
- Relative insensitivity to rotation noise
- Constraining of interpolation between flight lines* (important as all surveys are somewhat aliased across flight lines)
- Less importance of IGRF corrections (usually unnecessary)
- Direct indication of Euler structural index when combined with measurements of field
- Higher resolution than conventional TMI surveys—can be offset against survey height, allowing somewhat higher, therefore considerably safer, flying.

**not vertical TMI gradients*

Total field gradiometry versus tensor gradiometry. Total field gradient surveys are common (Hood, 1981) and while they share many of the advantages of tensor gradients such as obviating or reducing the need for base stations and regional corrections, total field gradients are not vectors or true potentials. Pedersen and Rasmussen (1990) discuss in some detail the practical problems encountered in the collection and processing of gradient tensor data. Christensen and Rajagopalan (2000) suggest that the next breakthrough in magnetic exploration is likely to be the measurement of the gradient tensor.

To examine how the total field gradient and the gradient tensor are related, denote the regional geomagnetic field vector by $\mathbf{F}$ and the local field vector by $\mathbf{F}'$. The anomalous field produced by subsurface sources is $\Delta\mathbf{B}$. Then

$$\mathbf{F}' = \mathbf{F} + \Delta\mathbf{B} \tag{1}$$

The measured total field anomaly is given by:

$$\Delta B_m = |\mathbf{F}'| - |\mathbf{F}| = \sqrt{(F_x + B_x)^2 + (F_y + B_y)^2 + (F_z + B_z)^2} - \sqrt{F_x^2 + F_y^2 + F_z^2} \tag{2}$$

Traditionally, this is assumed to equal the projection of the anomalous field vector onto the regional field direction, ΔB_T, where:

$$\Delta B_T = \Delta\mathbf{B} \cdot \mathbf{F} / F = \left(\Delta B_x F_x + \Delta B_y F_y + \Delta B_z F_z\right) / F \tag{3}$$

where $F = |\mathbf{F}|$.

ΔB_T has useful mathematical properties, because it is a potential field (it obeys Laplace's equation, as it is a linear combination of the components of $\Delta\mathbf{B}$, each of which obeys Laplace's equation) and can therefore be continued to other levels, if it is accurately known everywhere over one surface. In fact, the measured total field anomaly is equal to ΔB_T only to first order in $\Delta B/F$. When anomalies are strong (thousands of nanoteslas) the difference between the two "total field" anomalies becomes significant. An expression for the difference between the two measures of "total field anomaly" can

be obtained from equations 1-3:

$$\Delta B_m^2 = \left(F' - F\right)^2 = F'^2 + F^2 - 2F'F = 2F^2 + 2\Delta\mathbf{B}\cdot\mathbf{F} + \Delta B^2 - 2F'F$$
$$= 2\Delta\mathbf{B}\cdot\mathbf{F} + \Delta B^2 - 2F\left(F' - F\right) = 2F\Delta B_T + \Delta B^2 - 2F\Delta B_m$$
$$\therefore \Delta B_m = \Delta B_T + \frac{\Delta B^2 - \Delta B_m^2}{2F} \qquad (4)$$

It can be seen from equation 4 that the maximum error, for a given magnitude of the anomalous field vector $\Delta\mathbf{B}$, occurs when the anomalous field is oriented such that $\Delta B_m = 0$. For example, the difference between the two types of total field anomaly can be as large as 1000 nT for a 10 000 nT anomaly in a 50 000 nT regional field.

Whereas ΔB_T obeys $\nabla^2(\Delta B_T) = 0$ (Laplace's equation), from equation 4, the Laplacian of ΔB_m is given by:

$$\nabla^2\left(\Delta B_m\right) = \nabla^2\left(\Delta B_T\right) + \left(1/2F\right)\left[\nabla^2\left(\Delta B^2\right) - \nabla^2\left(\Delta B_m^2\right)\right]$$
$$= \left(1/2F\right)\left[\nabla^2\left(\Delta B^2\right) - \nabla^2\left(\Delta B_m^2\right)\right]$$

since $\nabla^2\left(B_T\right) \equiv 0$.

Writing the Laplacian in terms of components, it is easily shown that:

$$\frac{\partial \Delta B_x^2}{\partial x^2} = \frac{\partial\left(2\Delta B_x B_{xx}\right)}{\partial x} = 2\left[B_{xx}^2 + B_x\frac{\partial B_{xx}}{\partial x}\right] = 2\left[B_{xx}^2 + B_x\frac{\partial^2 B_x}{\partial x^2}\right]$$
$$\nabla^2\left(\Delta B_x^2\right) = 2\left[B_{xx}^2 + B_{xy}^2 + B_{xz}^2 + B_x\nabla^2\left(B_x\right)\right] = 2\left[B_{xx}^2 + B_{xy}^2 + B_{xz}^2\right]$$

since $\nabla^2\left(B_x\right) \equiv 0$.

$$\therefore \nabla^2\left(\Delta B^2\right) = 2\left[B_{xx}^2 + B_{xy}^2 + B_{xz}^2 + B_{xy}^2 + B_{yy}^2 + B_{yz}^2 + B_{xz}^2 + B_{yz}^2 + B_{zz}^2\right]$$

i.e., $\nabla^2\left(\Delta B^2\right) = 2\left[BXSIG^2 + BYSIG^2 + BZSIG^2\right]$

where *BXSIG* is the analytic signal derived from ΔB_x (i.e., calculated using tensor elements B_{xx}, B_{xy}, B_{xz}), etc., as in

$$BXSIG = \sqrt{B_{xx}^2 + B_{xy}^2 + B_{xz}^2} \qquad (5)$$

Similarly,

$$\nabla^2\left(\Delta B_m^2\right) = 2\left[\left(\frac{\partial\left(\Delta B_m\right)}{\partial x}\right)^2 + \left(\frac{\partial\left(\Delta B_m\right)}{\partial y}\right)^2 + \left(\frac{\partial\left(\Delta B_m\right)}{\partial z}\right)^2 + \left(\Delta B_m\right)\nabla^2\left(\Delta B_m\right)\right]$$
$$= 2\left[ANSIG^2 + \left(\Delta B_m\right)\nabla^2\left(\Delta B_m\right)\right]$$

where *ANSIG* is the analytic signal calculated from the gradients of ΔB_m in the *x*, *y*, and *z* directions:

$$ANSIG = \sqrt{\left(\frac{\partial\left(\Delta B_m\right)}{\partial x}\right)^2 + \left(\frac{\partial\left(\Delta B_m\right)}{\partial y}\right)^2 + \left(\frac{\partial\left(\Delta B_m\right)}{\partial z}\right)^2} \qquad (6)$$

Combining the above expressions and solving for $\nabla^2(\Delta B_m)$:

$$\left(1 + \Delta B_m / F\right)\nabla^2\left(\Delta B_m\right) = \left(1/F\right)\left[BXSIG^2 + BYSIG^2 + BZSIG^2 - ANSIG^2\right]$$
$$\therefore \nabla^2\left(\Delta B_m\right) = \frac{BXSIG^2 + BYSIG^2 + BZSIG^2 - ANSIG^2}{F'} \qquad (7)$$
$$\text{as } F' = F + \Delta B_m$$

The RHS of equation 7 is, in general, non-zero. For a body elongated parallel to *y*, $BYSIG^2 \approx 0$ and $BZSIG^2 \approx ANSIG^2$. Thus the $RHS \approx BXSIG^2/F > 0$. Because ΔB_m does not obey Laplace's equation exactly, it is not a potential field, and neither are its derivatives ($\partial\Delta B_m/\partial x$, $\partial\Delta B_m/\partial y$, $\partial\Delta B_m/\partial z$).

Measurement of the gradient tensor. The most appropriate sensors for gradient measurements are superconducting quantum interference devices (SQUIDs—see Foley et al., 1999 and Foley and Leslie, 1998). SQUIDs are small (a few cubic centimeters), low-power devices which may eventually find application downhole or in drones. Deployment of SQUIDs in aircraft and downhole present different problems. Platform stability will need to be addressed in aircraft—GPS, tilt meters, and other methods need to be assessed. Downhole instruments will have to be slim (<25 mm in diameter), robust, and reasonably affordable. SQUIDs potentially fulfill all these requirements.

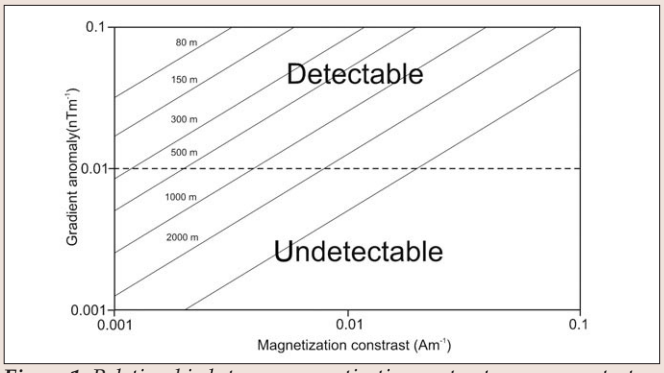

Figure 1. Relationship between magnetization contrast across a contact and the vertical gradient anomaly of the total field. The graph is divided into detectable anomalies and undetectable anomalies for various depths from 80-5000 m by the sensitivity level of 0.01 nT/m.

Table 1. *Anomalies of the gradient tensor element, B_{zz}, assuming RTP.*

Source (Euler index)	ΔB_z	ΔB_{zz} (h = 100 m)	ΔB_{zz} (h = 500 m)
Sphere n = 3	100 nT	-3 nT/m	-0.6 nT/m
	10 nT	-0.3 nT/m	-0.06 nT/m
Pipe n = 2	100 nT	-2 nT/m	-0.4 nT/m
	10 nT	-0.2 nT/m	-0.04 nT/m
Dyke n = 1	100 nT	-1 nT/m	-0.2 nT/m
	10 nT	-0.1 nT/m	-0.02 nT/m
Vertical contact n ~ 0.5	100 nT	-0.5 nT/m	-0.1 nT/m
	10 nT	-0.05 nT/m	-0.01 nT/m

SQUIDs detect minute changes of flux threading a superconducting loop. They are therefore variometers rather than magnetometers, but they are vector sensors since only changes perpendicular to the loop are detected. So-called high-temperature superconducting (HTS) SQUIDs operate at liquid nitrogen temperatures, overcoming the difficulties of handling liquid helium. The sensitivity of HTS SQUIDs is on the order of 100 fT (fT=10^{-15} Tesla) and it has been estimated that gradiometer sensitivity should be better than 0.01 nT/m, on a baseline of 10 cm (Peiselt et al., 2003).

Figure 1 shows the plotted relationship between magnetization contrast across a vertical contact and the vertical gradient anomaly of the total field, following Hood (1981). Although Hood's derivation is for total field anomalies over contacts, they are the same order of magnitude as gradient tensor elements. In addition, the consideration of anomalies over vertical contacts is conservative because the structural (Euler) index, *n*, of a contact is only ~0.5, whereas for a thin dyke $n = 1$ and for a dipole $n = 3$. These higher structural indices translate into larger gradient anomalies.

Additionally, Table 1 lists typical anomalies (assuming reduction to the pole for simplicity) of the gradient tensor element B_{zz}. If we consider a vertical contact between two paramagnetic rock units such as a mafic and a felsic gneiss, which contain no magnetite or pyrrhotite, with a susceptibility contrast of ~600 SI, at 100 m the vertical field anomaly ΔB_z is 15 nT while ΔB_{zz} is -0.08 nT/m. This should be easily detected by a gradiometer with a sensitivity of 0.01 nT/m.

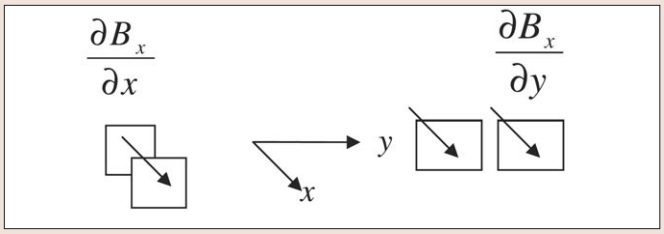

Figure 2. *Conceptual arrangement of SQUID sensors for detection of axial and transverse gradients.*

In regions which do not contain magnetic sources or significant time-varying electric fields, both the divergence and the curl of the magnetic field are effectively zero. This means that the magnetic gradient tensor is symmetric and traceless. The first property means that only three of the transverse (off-diagonal) tensor elements are required to be measured while the second property means that only two of the axial (diagonal) elements are required. Overall we only need to measure five tensor elements. Figure 2 depicts an arrangement of SQUID sensors for the detection of axial and transverse gradients. Detection of axial gradients requires two separate SQUID sensors, but each transverse gradient can be detected using a single planar sensor, which greatly simplifies the total package. Thus, for this arrangement, seven SQUIDs are required in all to measure the magnetic gradient tensor.

In reality there are problems using SQUIDs statically that are beyond the scope of this article to address. It is far more effective to use rotating sensors to overcome *1/f* noise and the problem of SQUIDs unlocking (see Schmidt et al., 2004).

Specific advantages of magnetic tensor gradiometry. Benefits that are specific to gradient tensor surveys include:

- Magnetic tensor gradiometry provides the benefits of vector surveys without the disadvantage of extreme sensitivity to orientation.
- Tensor elements are true potential fields, with desirable mathematical properties (important in areas with strong anomalies), allowing rigorous continuation, RTP, magnetization mapping, etc.
- Very rapid sampling rate of SQUID sensors allows unaliased detection of high-frequency aircraft noise and efficient removal by filtering—total field magnetometers have much slower sampling, causing compensation problems.
- Redundancy of tensor components gives inherent error correction and noise estimates.
- Wide range of new types of processed data are possible: Invariants, directional filters, depth slicing, source moments, and dipole location are unaffected by sensor misorientation.
- Invariant quantities exist that have higher resolving power than the analytic signal (Pedersen and Rasmussen, 1990).
- Allows direct determination of 3D analytic signal (defines source outlines; width/depth determinations—irrespective of remanent magnetization).
- Each tensor component represents a directional filter, emphasizing structures in particular orientations.
- Measurement of tensor allows calculation of parameters with superior resolving power to conventional analytic signal.
- Measurement of tensor allows calculation of parameters unaffected by aliasing across flight lines.
- Superior Euler deconvolution solutions from measured tensor elements with improved accuracy using true measured gradients along and across lines.
- Tensor elements are independent of skewing caused by geomagnetic field direction—ease of interpretability.
- Combination of tensor components gives information on magnetization directions.
- Measurement of full tensor allows rotation of coordinate system, yielding transformed tensor components that emphasize specified structural orientations.
- Direction to compact source is defined directly from single station measurement.
- Direct calculation of compact source magnetic moments is possible.
- Improved resolution of pipe-like bodies.
- Improved resolution of sources subparallel to flight path.
- Improved delineation of N-S elongated sources in low latitudes.
- Spinoff applications to downhole magnetics and remote determination of source magnetic properties in situ.

Characteristics of tensor gradient components and derived quantities. In the following, the conventions used are: $+x = N$; $+y = E$; $+z$ = down.

- B_{xx} delineates E-W boundaries preferentially (symmetric for vertical magnetization, antisymmetric for horizontal magnetization).
- B_{yy} delineates N-S boundaries preferentially (symmetric for vertical magnetization, antisymmetric for horizontal magnetization)
- B_{xy} delineates body corners preferentially (anomaly signs depend on magnetization direction).
- B_{zz} delineates steep boundaries preferentially (symmetric for vertical magnetization; antisymmetric for horizontal magnetization).
- B_{xz} delineates E-W boundaries preferentially (antisymmetric for vertical magnetization; symmetric for N-S horizontal magnetization).
- B_{yz} delineates N-S boundaries preferentially (antisymmetric for vertical magnetization; symmetric for E-W horizontal magnetization).
- The B_{ij} can be rotated into another coordinate system to resolve specific structural orientations.
- Because B_{xz} and B_{yz} are acquired over a quasi-horizontal surface, they can be differentiated numerically to obtain $\partial B_{xz}/\partial x$ and $\partial B_{yz}/\partial y$. The second vertical derivative of ΔB_z, which has higher resolution than the first vertical derivative (B_{zz}), is easily calculated from these quantities:

$$B_{zzz} = \partial^2(\Delta B_z)/\partial z^2 = -\partial B_{xz}/\partial x - \partial B_{yz}/\partial y \qquad (8)$$

- The invariant I_1 outlines source boundaries and appears to have superior resolving power to the analytic signal. This is understandable, because of its faster falloff rate with distance.

$$I_1 = B_{xx}B_{yy} + B_{yy}B_{zz} + B_{zz}B_{xx} - B_{xy}^2 - B_{yz}^2 - B_{zx}^2 \qquad (9)$$

- The invariant I_2 preferentially outlines shallower features of complex sources, due to its higher fall-off rate than I_1.

$$I_2 = DET\left[B_{ij}\right] = B_{xx}\left(B_{yy}B_{zz} - B_{yz}^2\right) + B_{xy}\left(B_{yz}B_{xz} - B_{xy}B_{zz}\right) + B_{xz}\left(B_{xy}B_{yz} - B_{xz}B_{yy}\right) \qquad (10)$$

The superior performance of the invariant I_1 is clearly shown in Figure 3 which compares the *ANSIG* and I_1 for a vertical prism model with vertical down (remanent) unit magnetization at the (magnetic) equator. The *ANSIG* fails to detect the north-south sides of the prism, giving the appearance of two distinct bodies, while I_1 not only reveals these boundaries

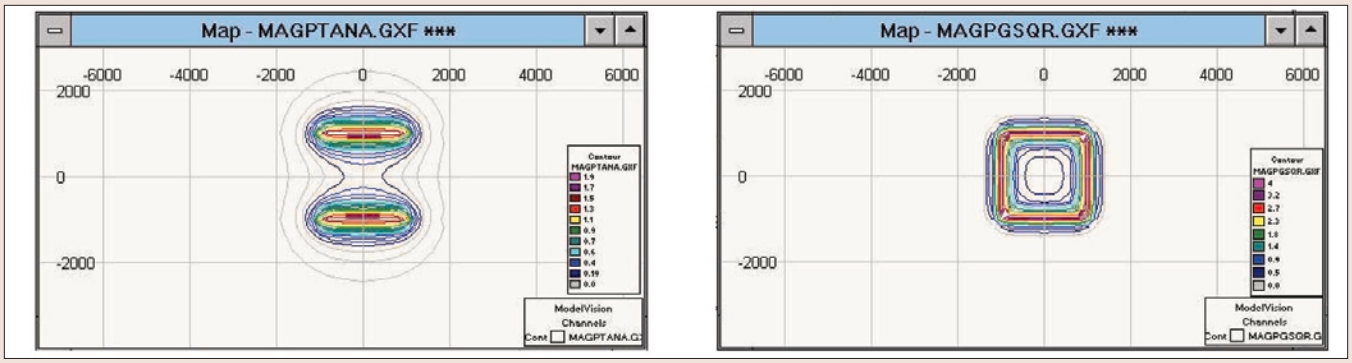

Figure 3. *Comparison of ANSIG (left) and I_1 (right) for a vertical prism model with vertical down (remanent) unit magnetization at the (magnetic) equator.*

but also resolves them with greater clarity. Although the geometry chosen here is extreme it is emphasized that remanence should never be ignored and it is highly likely that somewhere in all surveys these or similar geometries exist.

Combined tensor/vector magnetometer packages. The tensor components along a short segment of a survey line or drill hole are sufficient to determine the location and magnetic moment of a compact (quasi-dipolar) source uniquely. There is insufficient information in the gradient of the total field $\nabla(\Delta B_m)$ to solve for these parameters. A tensor gradiometer sensor package could record field components (i.e., ΔB), as well as the gradients of these components, which would also allow direct determination of compact source location and moment.

Although small pods or veins of strongly magnetic material adjacent to a drill hole will produce intense gradients, the fall-off rate is very rapid. This implies:

- Small magnetic bodies not in the immediate vicinity of the hole produce negligible effects.
- Pockets of magnetic material adjacent to the hole produce very localized spikes, easily distinguishable from the smoothly varying signature of large off-hole sources, particularly when combined with vector data.

A combined tensor/vector magnetometer package would allow the remote determination of in-situ magnetic properties of sources from the surface or subsurface, using natural geomagnetic variations, without the alignment problems that afflict the differential vector magnetometer method (Clark, 1997; Clark et al., 1998).

Conclusions. There are many reasons why gradient tensor measurements will improve the interpretability of magnetic surveys, especially in areas where anomaly patterns are skewed by remanence or low magnetic latitudes. Gradient tensor surveys retain the benefits of vector surveys without the disadvantage of extreme orientation sensitivity. The tensor elements are true potential fields with desirable mathematical properties. The tensor formulation opens up a wide range of new types of data processing, including tensor Euler deconvolution, eigenvalue/vector relationships, invariants, directional filters, depth slicing, source moments, and dipole location unaffected by sensor misorientation.

The crucial difference between full-tensor gradiometry and total field gradiometry is the production of more detailed and quantitatively interpretable maps and 3D models, rather than simple bump (scalar anomaly) detection. Magnetics is still the cheapest and most widely used geophysical mapping tool in hard rock environments, with increasing importance and potential for further growth in hydrocarbon exploration.

If sensitivities of 0.01 nT/m can be achieved then even anomalies over vertical contacts (structural index ~0.5) between bodies with a susceptibility contrast as low as 600 SI can be detected at depths of over 100 m. 600 SI is a very low susceptibility contrast. Obviously anomalies over bodies with greater susceptibilty contrasts and/or higher structural indices can be detected at greater depths.

Tensor gradiometry will prove useful for aeromagnetic surveys with wide line spacings (e.g., over sedimentary basins), environmental surveys, defense applications such as submarine and unexploded ordnance detection, downhole magnetics, and for marine surveys. Any substantial improvement in this technology will have enormous benefits in terms of new discoveries and lower exploration costs.

Suggested reading. "The magnetic vector and gradient tensor in mineral and oil exploration" by Christensen and Rajagopalan (Australian Society of Exploration Geophysicists *Preview*, 2000). "Theory of differential vector magnetometry—a new method for remote determination of in situ magnetic properties and improved drill targeting" by Clark (*Exploration and Mining*, 1997). "Remote determination of magnetic properties and improved drill targeting of magnetic anomaly sources by differential vector magnetometry (DVM)" by Clark et al. (*Exploration Geophysics*, 1998). "Potential use of high Tc SQUIDs for airborne electromagnetics" by Foley and Leslie (*Exploration Geophysics*, 1998). "Field trials using HTS SQUID magnetometers for ground-based and airborne geophysical applications" by Foley et al. (*IEEE Transactions on Applied Superconductivity*, 1999). "Aeromagnetic gradiometry: A superior geological mapping tool for mineral exploration programs" by Hood (in proceedings of SQUID Applications to Geophysics, SEG workshop, 1980). "The gradient tensor of potential field anomalies: Some implications on data collection and data processing of maps" by Pedersen and Rasmussen (GEOPHYSICS, 1990). "High-Tc dc-SQUID gradiometers in flip chip configuration" by Peiselt et al. (*Superconductor Science and Technology*, 2003). "Can we estimate total magnetization directions from aeromagnetic data using Helbig's integral equations?" by Phillips (*Earth, Planets and Space*, 2005). "Directions of magnetisation and vector anomalies derived from total field surveys" by Schmidt and Clark (Australian Society of Exploration Geophysicists *Preview*, 1997). "The calculation of magnetic components and moments from TMI: A case study from the Tuckers igneous complex, Queensland" by Schmidt and Clark (*Exploration Geophysics*, 1998). "Advantages of measuring the magnetic gradient tensor" by Schmidt and Clark (Australian Society of Exploration Geophysicists *Preview*, 2000). "GETMAG—A SQUID magnetic tensor gradiometer for mineral and oil exploration" by Schmidt et al. (*Exploration Geophysics*, 2004). TLE

Corresponding authors: phil.schmidt@csiro.au, david.clark@csiro.au